

Calligraphic Poling for WGM Resonators

Makan Mohageg, Dmitry Strekalov, Anatoliy Savchenkov, Andrey Matsko,
Vladimir Ilchenko, Lute Maleki
Jet Propulsion Lab, 4800 Oak Grove Drive, Pasadena, CA, USA 91109

ABSTRACT

By engineering the geometry of a nonlinear optical crystal, the effective efficiency of all nonlinear optical oscillations can be increased dramatically. Specifically, sphere and disk shaped crystal resonators have been used to demonstrate nonlinear optical oscillations at sub-milliwatt input power when cw light propagates in a Whispering Gallery Mode (WGM) of such a resonant cavity. In terms of both device production and experimentation in quantum optics, some nonlinear optical effects with naturally high efficiency can occult the desired nonlinear scattering process. The efficiency of second order nonlinear optical effects in ferroelectric crystals can be increased by engineering a poling structure to the crystal resonator. In this paper, I will discuss a new method for generating poling structures in ferroelectric crystal resonators called *calligraphic poling*. The details of the poling apparatus, experimental results, and speculation on future applications will be discussed.

Keywords: PPLN, Nonlinear Optics, WGM, microsphere

1. INTRODUCTION

Constructing periodically poled LiNbO₃ (PPLN) structures is of great importance in nonlinear optics and quantum optics. Optical parametric oscillators [1-3], Bragg reflectors [4], second harmonic generators [5,6], photonic bandgap devices [7], and the generation of squeezed light [8] have all been demonstrated with PPLN.

The process of poling LiNbO₃ causes a localized reversal in the direction of the permanent electric polarization of the crystal. Techniques involving wet etching and photolithographic preformed masks [9-11] have been used for poling purposes. These methods, while readily applicable to multiplicative reproducing of simple domain patterns, such as linear gratings, are not convenient for the real time generation and visualization of patterns of arbitrary shapes, as required in some fundamental applications [13], because the technique requires the fabrication of the photolithographic mask each time as the domain map changes.

A technique to pole thin LiNbO₃ crystals while monitoring the growth of domain walls *in situ* has been developed and is discussed in this paper, with specific application to WGM resonators. Although the technique is general and can be applied to 180-degree ferroelectrics of any geometry. This technique is called *calligraphic poling*, for rather than charging a preformed mask, a micron sized needle that drags charge across the surface of the crystal causes domain reversal in real time. The shape of the resulting reversed domain is then given by the trajectory of the tip of the needle, with any breaks introduced by switching the voltage off as desired.

There are some advantages of calligraphic poling when compared to traditional approaches. This method is flexible and allows generating an arbitrary complex domain pattern on a crystal without the fabrication of an expensive mask. The poling process can be observed optically and manipulated in real time. This method does not require extreme environment conditions and domain reversal in samples of thickness less than 200 microns occurs fast enough to make calligraphic poling practical. The entire process takes place on a tabletop, at room temperature and at atmospheric pressure. Further, all poling patterns are reversible, that is, the poling structure on a particular crystal can be erased and a new one inscribed without significant alteration of the poling apparatus. This aspect is very important for independent

research labs, since it allows some freedom to test poling structures before using a preformed mask to mass produce them.

We demonstrate complex domain structures with two types of poling patterns: smooth curves and hexagons. The smooth curves are fabricated when a micron thick needle electrode moves across the top surface crystalline wafer, while the hexagons are generated when the tip of the electrode is stationary for some amount of time. Narrow domains less than 2 μm across are fabricated either as straight, smooth lines or as curves across the single-domain crystal. Selection of electrode material, radius, and inclination are important factors, and are all discussed later.

Changes to the poling process due to alignment of the needle electrode with the crystal x and y axes have not been observed. Domains in the shape of hexagons (as determined by the crystal structure of LiNbO_3) are readily obtained. Previous demonstrations of hexagon poling have involved creating a preformed mask with hexagons, then carefully aligning the stencil's hexagon vertices to the x - and y - directions of the crystal before applying voltage. With calligraphic poling, hexagon formation is automatic. Hexagon poling is interesting because it allows for the creation of two dimensional photonic and microwave bandgap devices.

With more development, observing the growth parameters of hexagonally shaped domain structures could be used to nondestructively study crystal purity. For example, we have observed symmetric hexagon generation in stoichiometric material and asymmetric hexagon generation in congruent material.

We verified our technique for congruent crystals that are less than 200 μm thick and stoichiometric crystals less than 250 μm thick. We found that inhomogeneities in crystal composition play a decidedly large role in the poling process. Both the domain growth rate and the minimum poling voltage depend on location on the crystal surface where the tip electrode is applied. In general, real-time control of bias voltage and time of interaction (described in detail below) can be used to ensure precision generation of a desired poling pattern.

2. CALLIGRAPHIC POLING

2.1 The apparatus

The calligraphic poling machine consists of a sharp edged tungsten electrode (needle) that brushes across the surface of the crystal. The crystal is in turn mounted on a flat polished electrode. Between the crystal and the flat electrode (the substrate) is a micron thin layer of conducting liquid to ensure uniform conductance for all points on the crystal. Depending on configuration, either the substrate or the needle is attached to some computer controlled translation/rotation stages to change the position of one with respect to the other. By applying a bias voltage between the needle and the substrate, domain structures are drawn directly onto the crystal in a user or computer defined pattern. A cartoon of the calligraphic poling machine is shown in Fig. 1. A picture of the device calligraphic poling machine we use is shown in Fig. 2.

The needle electrodes we use are the same component as the probes used in atomic force microscopy. We found that needle electrodes made of a solid shank of tungsten are better suited for calligraphic poling than bent electrodes with 'cat-whisker' tungsten tips, cut copper wire, or the edge of a razor. When the radius of the tip of the needle is smaller than half a micron, the lifespan of the tip is shorter than the time it takes to complete a typical poling pattern. Similarly, needles made of copper will gradually become dull and possibly bend after only a few poling cycles. Since the pen is in physical contact with the upper surface of the crystal, excessive pressure applied may cause either the crystal or the pen to break. Using a razor will usually cause a crack to form in the crystal, while the whisker-like tip will certainly

bend and break under even modest strain. Using the crimped end of a piece of copper wire is an attractive choice for engineering narrow domain structures. However, the lack of rigidity in copper wires allows for hysteresis in motion and uncontrollable slipping when this sort of pen is moved.

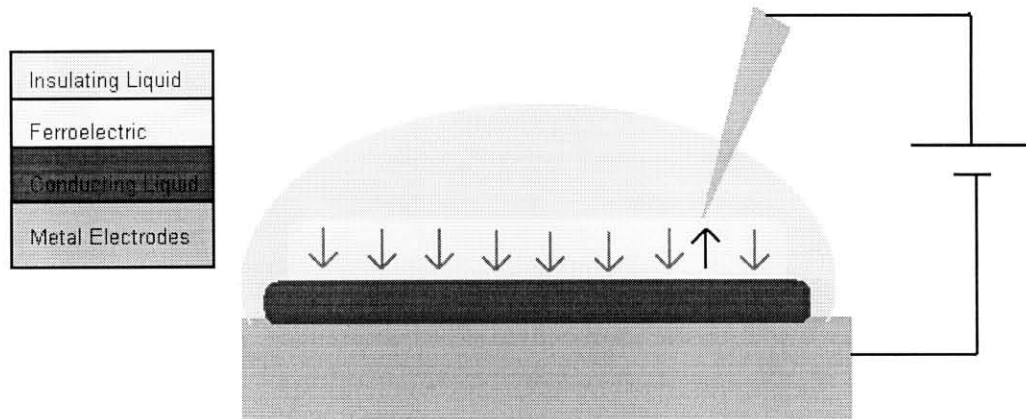


Fig. 1: Diagram of the calligraphic poling machine. The needle is free to move across the surface of the crystal. When voltage is applied, domain reversal takes place locally under the position of the tip of the needle. The arrows represent the direction of the polarization for local regions on the crystal.

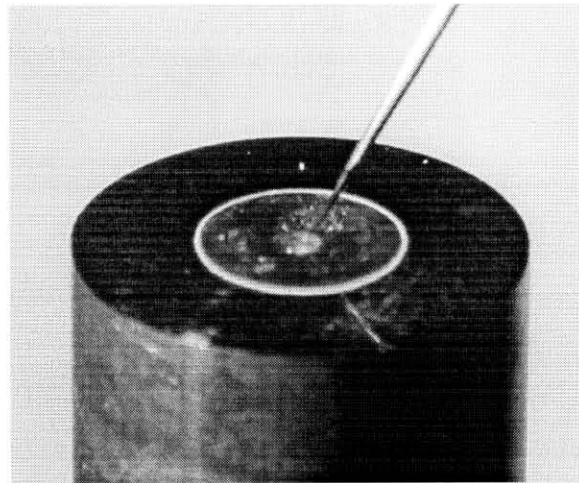


Fig. 2: Picture of our calligraphic poling machine. The substrate used here is 1.26 cm diameter piece of brass that has been hand polished.

Choosing the appropriate solid tungsten probe is critical. It was found that pen electrodes of 1 μm radius work best. Larger radius pen electrodes automatically exclude straightforward engineering of small domains. Smaller radius pen electrodes initially allow for smaller domain structures. However, after some time, the stress of dragging the pen across the surface of the crystal will cause the pen electrode to bend. Charge build up will cause domain flipping to occur along the position of the bend in the electrode instead of at the tip of the electrode, or both.

The lower surface of the crystal is placed into contact with a polished flat electrode (the substrate). A thin layer of conducting liquid, for example salt water, is placed between the substrate and the crystal to ensure uniform electrical contact between the two nearly-flat surfaces. Furthermore, a thin layer of salt water serves as a strong binding agent between the crystal and the substrate. The salt water keeps the crystal from moving around while the poling process takes place.

Two different materials were successfully used as the substrate. The thin plate of a metallic mirror was initially chosen because of its excellent surface quality. However, stress, strain, and the occasional spark can cause cracks to form on the thin metal surface which may insulate different parts of the substrate surface. Because of this recurring issue, a solid piece of brass with one polished surface was used as the substrate instead of the metallic mirror. Scratches and cracks along the surface do not result in electrical isolation because of the thickness of the substrate and the salt water coating. However, surface defects deeper than several dozen microns can collect dust particles and other contaminants which cause sparking at lower voltages than that which is required for domain reversal.

2.2 Poling dynamics

The size and shape of the domains produced by calligraphic poling are controlled by the magnitude of the voltage bias between the needle and the substrate, the duration of the applied voltage, the quality of the crystal, and the thickness of the crystal. Typically, high voltage bias, from 2—3 kV, applied over time periods less than 2 s to a motionless pen yield hexagons; while intermediate voltages (800 V—1.8kV) applied over longer time periods to a moving pen yield straight lines and curves. Crystal thickness also affects the poling dynamic. We observed that the resultant domains in a thick crystal are smaller than those of a thin crystal when applied to the same voltage for the same amount of time. Fig. 3 and Fig. 4, which are adapted from [14], present some typical results achieved with the poling process.

Stoichiometric crystals, that is, crystals that have a ratio of Li to Nb that is near unity, show domain reversal at much lower voltages—typically at or around 400 V for a crystal of the same thickness described above. Poling stoichiometric crystals results almost exclusively in hexagonal shaped domain patterns.

Note that the values for required voltages reported in this article for both congruent and stoichiometric material do not correspond with the same values discussed elsewhere. In all other experiments, the polarization of a large region of a single domain crystal was being reversed, while with calligraphic poling only a small portion of the crystal is exposed to the bias field, thus some amount of screening is expected. We should point out that while the data presented in Figures 3 and 4 are typical of calligraphic poling, and the description of poling dynamic given in this section is mostly representative of actual behavior, each individual crystal sample apparently has slightly different poling dynamics. These properties must be quantified before poling begins. For instance, a few 'test domains' could be applied to the crystal and their size and shape can be verified by the visualization technique described below.

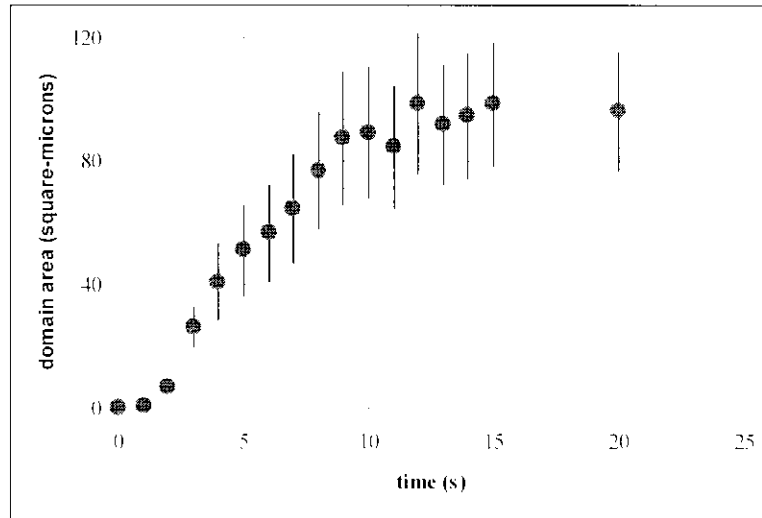
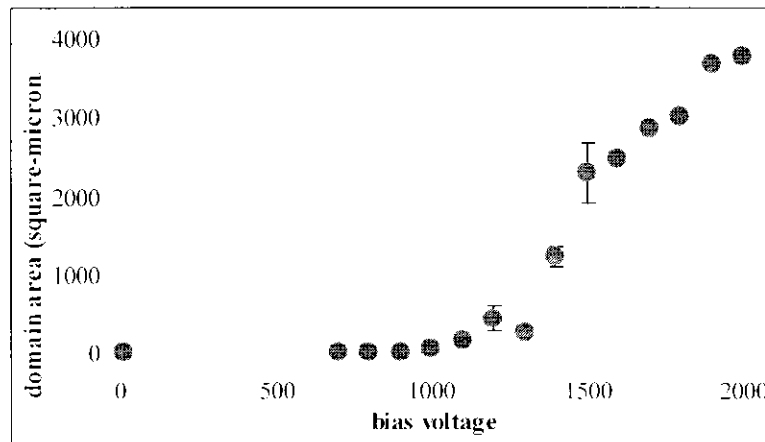
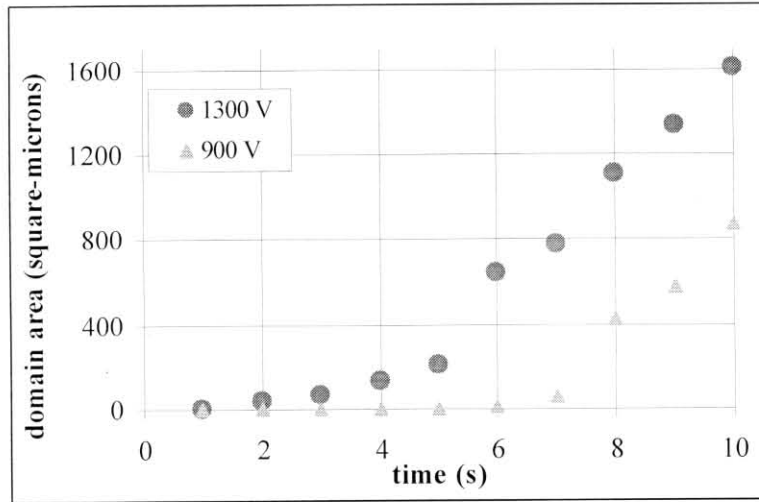


Fig. 3: poling dynamics of a 200 μm thick specimen of congruent LiNbO_3 . 3 kV of bias was applied through a 1 μm tungsten pen and the surface area of the resultant domain structure was recorded. This experiment was repeated nine times at various locations on the crystal to obtain the error bars.

The poling dynamics for congruent and stoichiometric LiNbO_3 through calligraphic poling are different. Fig. 3 shows dynamics data for poling congruent LiNbO_3 . Fig. 4 shows the same type of data for stoichiometric LiNbO_3 . Each data point is an average of 5 points taken with the same parameters on different regions of the same crystal to average out any differences in structural content of the crystal. The behavior shown in these data sets, while not conclusive, indicates some threshold behavior for the poling dynamic in both types of crystal.



(a)



(b)

Fig 4: poling dynamics in 200 μm thick stoichiometric LiNbO_3 . (a) Increasing bias voltage applied to different regions of the crystal for 5 s results in domain structures of increasing size. (b) Increasing the time a given bias voltage is applied will result in domains of increasing size.

An advantage of calligraphic poling is the ability to erase a poled structure on a crystal. We found some curious phenomena in the process. For example, Fig. 5 shows how the domain size may depend on the poling history of the crystal. A domain was created at some voltage applied for some time. The size of the domain was measured using the non-destructive visualization technique discussed in this article. The domain was then erased by inverting the sign of the applied field. After erasure, the same voltage was applied over the same amount of time to the same spot of the crystal. The size of the new domain was measured, and then it was erased again. This process was repeated for several iterations. The oscillations observed in the measured domain size in congruent samples could be attributed to a work-hardening analogue in ferroelectric domain reversal, or some dependence of bias voltage on stress in the crystal, or perhaps even a sort of electrostatic annealing analogue, though we do not have an explanation for the observed phenomenon.

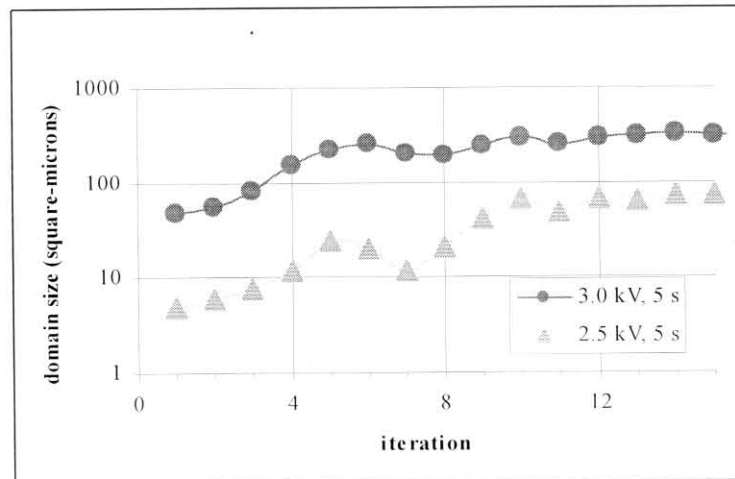


Fig. 5: Ferroelectric work-hardening in congruent LiNbO_3 . Domains are flipped, erased, and re-poled in successive iterations. The measured surface areas of the domains grow dramatically through several iterations.

2.3 Domain visualization

Visualization of the domains can be an intrinsic part of the calligraphic poling process. Light incident from above the crystal (+z-direction) reflects off of its bottom surface. As the voltage between the top and bottom surfaces is increased, the gradient in the refractive index of the narrow region between +z and -z poled regions (the domain wall) increases. This results in distinct dark lines that outline regions of domain inversion, which are visible with the aid of an optical microscope. Note that unlike the conventional techniques that rely on polarization changes of light, polarizer/analyzer elements are not required for the visualization of the domains. Fig. 6 shows the visualization of a radial-spoke shaped domain structure applied via calligraphic poling techniques.

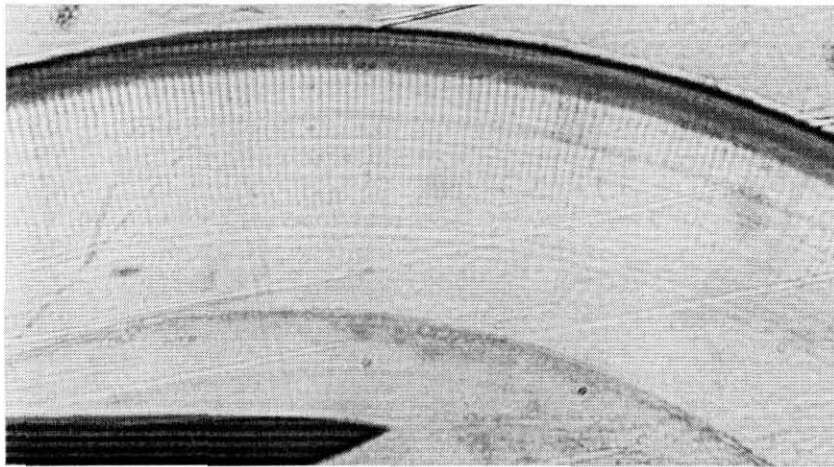


Fig. 6: (a) a radial poling pattern 10 μm thick, several hundred microns long that follows the circumference of a disk shaped crystal. The silhouette of the needle electrode points towards the edge of the disk. These images appear orange because of the brass substrate used as the bottom electrode.

Since domains are visualized as they are generated with the high voltage bias applied between the needle and the smooth substrate, calligraphic poling allows *in situ* monitoring of the domain growth process. Domain visualization occurs at far lower voltages than those required for domain reversal, however. The minimum voltage required to observe preexisting domain patterns, approximately 200 V, is only a fraction of the voltage required to cause domain reversal to occur, thus the visualization technique is non-destructive. This value is a function of the surface quality of the crystal and substrate. To verify that domain flipping has taken place through the depth of the crystal, the crystal is flipped over and the same pattern is verified on the opposite side of the crystal. Fig. 7 shows the visualization of hexagon-shaped domain structures achieved through calligraphic poling.

Once the domain pattern is formed, it can be visualized under magnification while the crystal sample is heated. In the case of radially poled disks (as shown in Fig. 5), viewing the disk in the radial direction and focusing slightly off-center shows domains without temperature or voltage bias. This is because of the birefringence of the material.

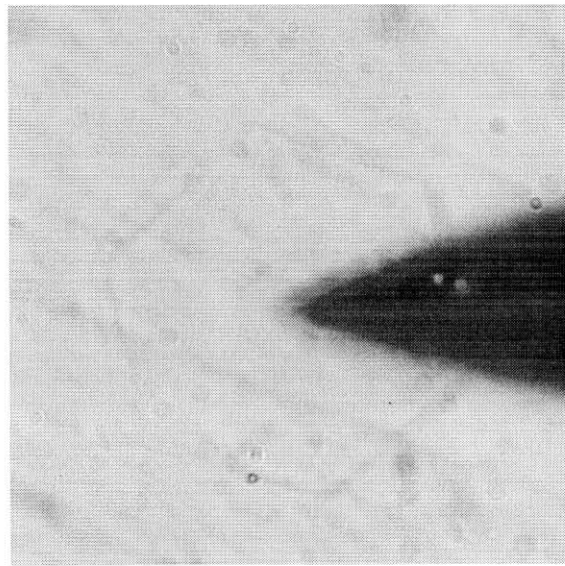


Fig.7: (a) A hexagonally shaped domain pattern in stoichiometric LiNbO_3 24 μm edge to edge visualized ex situ. The large black arrow is the silhouette of the needle used for writing and visualizing the domain.

2.4 Poling near edges and other discontinuities

Poling near discontinuities and edges is possible with calligraphic poling so long as the appropriate precautions are taken. Edge poling requires the crystal and needle to be immersed in an insulating oil because placing the pen, e.g., within 100 μm of the edge of the crystal causes at best no domain reversal, and at worst sparking that can result in the destruction of the crystal and the pen. If an insulating oil of sufficiently large dielectric constant is used, poling up to the very edge of a polished crystal can be achieved [14].

The steps for poling close to the crystal edges are the following. First, the crystal surface must be free of any scratches, cracks, or holes. This is visually verified by use of a microscope, and physically achieved by polishing or by any other means.

Second, the substrate in electrical contact with the lower surface of the crystal is polished to be cleared of all scratches. Any sharp points or discontinuities in its surface will cause an inordinate amount of charge to build up and result in a dramatic spark that can move or damage the crystal specimen. Using a metallic mirror as the substrate or polishing the substrate with a diamond paper are simple ways to ensure a smooth substrate.

Once these steps are complete, a thin layer of saltwater is placed between the lower crystal surface and the smooth electrode. Over time, the weight of the crystal will squeeze out all but a thin film of the saltwater. This thin film will hold the crystal in place and keep out any other substance between the crystal and the lower substrate. Then, a hydrophobic insulating dielectric oil is added to cover the crystal and smooth electrode, as in Fig. 8. After enough time is given for all the excess salt water to leave the gap between the crystal and the substrate, the insulating oil surrounds the upper and edge surfaces of the crystal. The needle, which drags along the top surface of the crystal, causes charge to build up at its tip when a voltage is applied between the pen and the substrate. Since the crystal specimen is immersed in an insulating bath, the charge will continue to build up until an amount of charge sufficient for domain reversal is generated. Once this condition has been met, the permanent polarization of the region of the crystal immediately underneath the pen is reversed, causing a pulse of current to flow in the circuit.

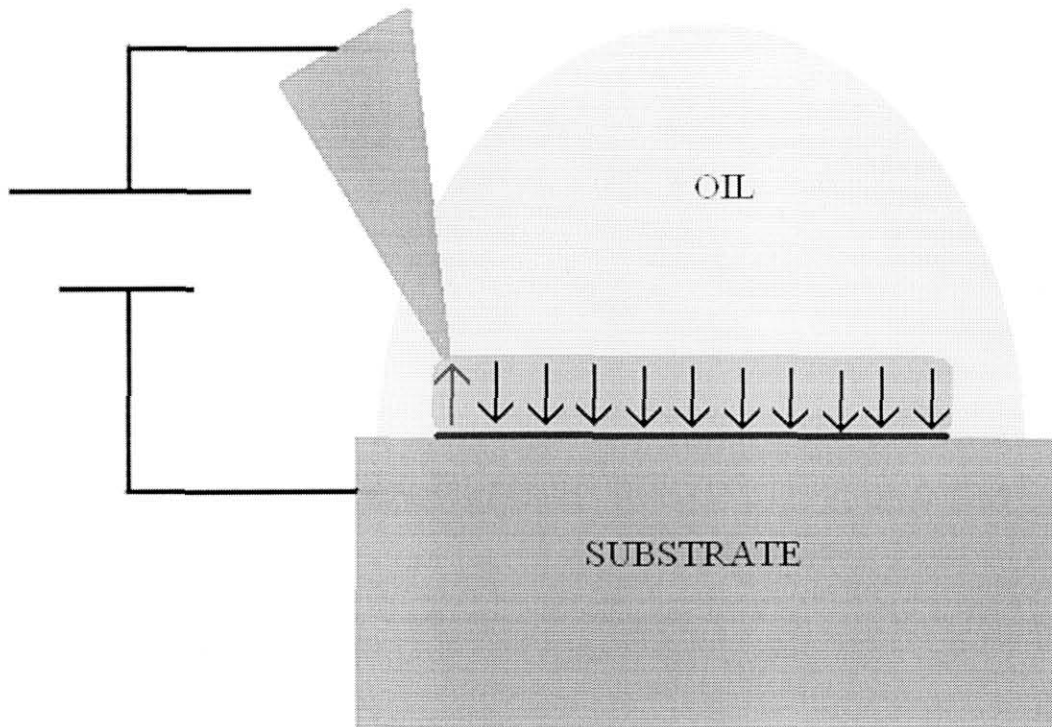


Fig. 7: Modification to the calligraphic poling machine to allow for edge-poling on a polished crystal. A hydrophobic, transparent, and insulating oil prevents sparks from charge build up on the edge of the crystal.

Any oil or other material is cleared off from the calligraphic poling apparatus before the crystal is removed. Dousing the specimen in alcohol, then distilled water, and then acetone clears off most of the contaminants introduced in the calligraphic poling process. To remove the crystal, a single drop of salt water is placed near the edge. This drop will combine with the thin film of water underneath the crystal and cause a bead to form underneath the crystal, gently separating it from the substrate.

3. EXPERIMENTAL RESULTS

A poling structure reminiscent of concentric rings was used to tune the optical spectra of a LiNbO_3 WGM resonator. All modes in such a resonator have radially dependant wave functions. Higher order modes have radial maxima closer to the disk edge, while lower order modes have maxima closer to the disk center. In a resonator with a ring shaped poling pattern, modes of different radial orders will mostly occupy regions of the cavity with different polarization, as illustrated in Fig. 8. Fig. 9 shows an experimental realization of such a poling pattern, and is adapted from [15].

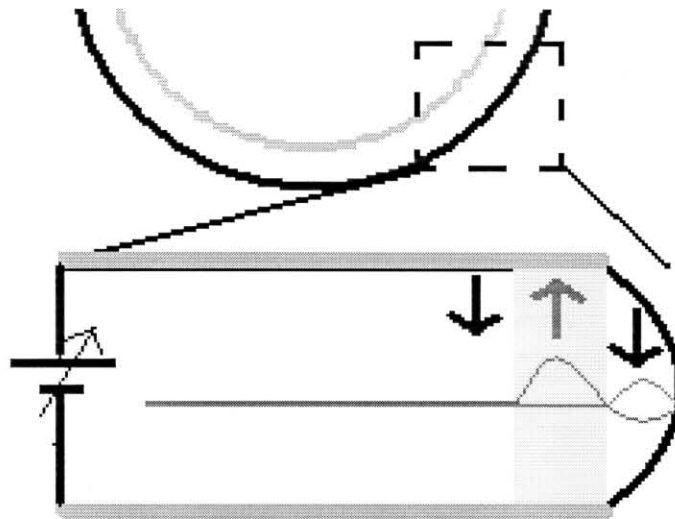


Fig. 8: (top) a ring shaped poling pattern on a disk shaped resonator (bottom) a cross sectional view of the cavity with an indication of the radial dependence of two eigenmodes of the cavity.

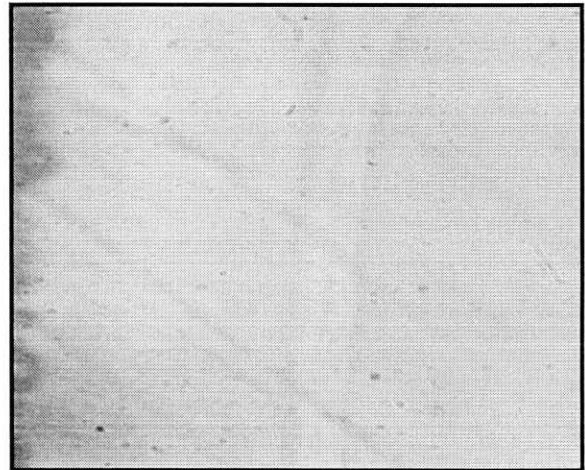
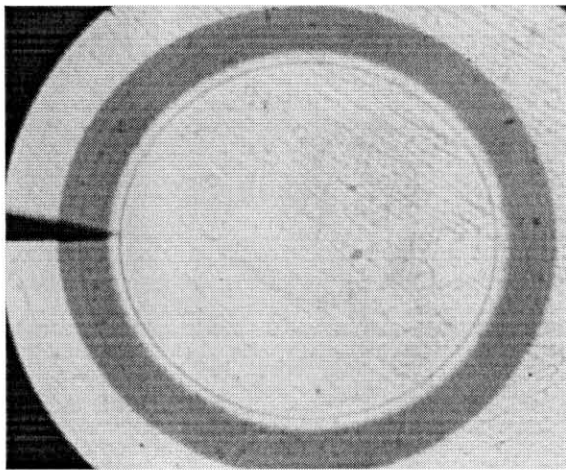


Fig. 9: Left: a disk with a ring shaped poling pattern some 10 microns from the disk edge. Right: detail of the poling pattern, which is a ring 2 microns edge-to-edge.

Applying a voltage bias across the resonator causes the refractive index of each region to change in different directions (that is, to increase or decrease) through the Pockells effect, which means the frequency of modes will change based on their radial wavenumber. Through careful engineering, the frequency of a single family of ‘radical’ modes can be shifted with respect to the rest of the modes in the resonator. We achieved, what is to our knowledge a first demonstration of this effect, with a tunability of $20 \text{ MHz}/V_{\text{bias}}$. Experimental results of the frequency tunability are shown in Fig. 10.

This type of device forms the critical element of a tunable optical filter, and could also be used as a component in an optical cavity with tunable FSR or perhaps a single sideband optical modulator.

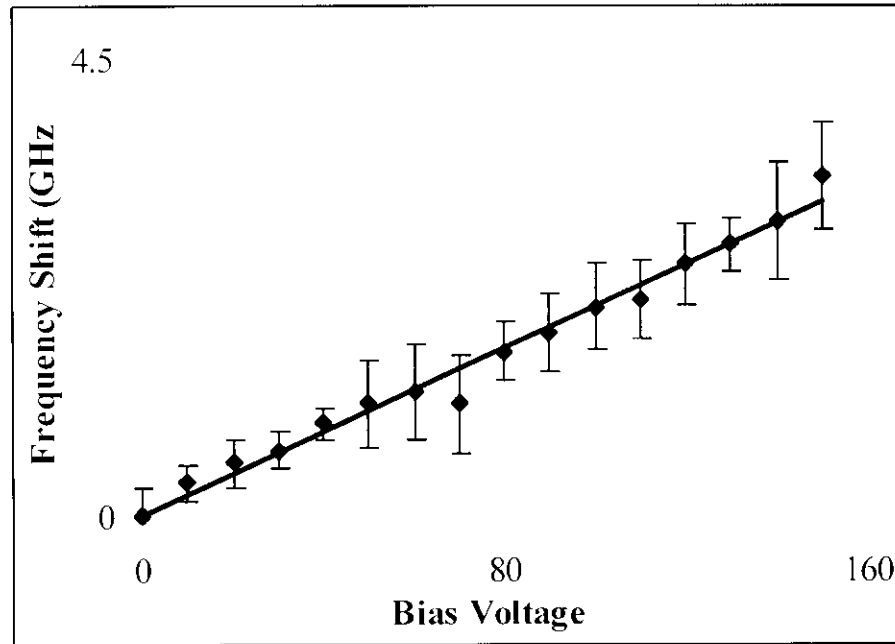


Fig. 10: Tuning the frequency of one mode in the resonator spectra while keeping the frequency of other modes static.

Increasing the efficiency of optical SHG and optical parametric oscillations (OPO) in general is a common goal among practitioners of nonlinear optics. The high Q-factor of WGM resonators implies that large field intensities are achievable with small input powers. For any scattering process to occur, energy and momentum must be conserved. For a process like second harmonic generation or sum/difference frequency generation, energy is conserved, but dispersion in the material means momentum (phase) is not conserved. To compensate for this, a periodic modulation in the sign on the second order nonlinear optical coefficient is needed to quasi-phase match pump, signal and idler waves. Physically, a linear grating formed by adjacent up and down poled domains approximates the required periodic modulation. For WGM resonators, the traditional linear grating is 'bent' around the circumference of the disk resonator, forming a set of daisy-petal like radial domains, as shown previously in Fig. 6.

The step size depends on the index mismatch between pump, signal, and idler waves. Because of the large optical fields that exist in WGM cavities, the refractive indices may change as a function of input intensity as well. Temperature fluctuations also cause shifts in refractive index. Furthermore, changes to the poling period from geometric dispersion must be considered for small radius disks. Without using extensive control apparatus, a linearly chirped poling structure can account for some of the fluctuations in refractive index mismatch.

SHG has been observed in WGM resonators with a radial poling structure chirped linearly from 14 microns up to 40 microns step size. A large chirp in the poling structure allows for broadband frequency conversion at low efficiency, as shown in Fig. 11. Reducing the chirp reduces the range of SHG while increasing the overall efficiency.

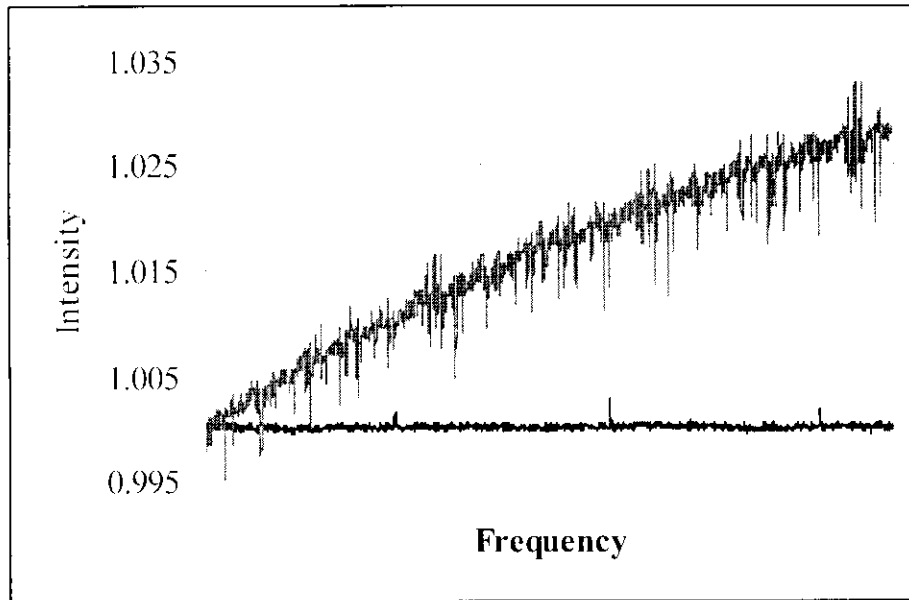


Fig. 11: Pump (upper spectra) at 1550 nm is converted to SH (lower spectra) at 775 nm.

4. DISCUSSION

Calligraphic poling is a low cost, and easy to implement technique for domain engineering LiNbO_3 and possibly other ferroelectrics. The general operational parameters of calligraphic poling are described and several examples of experimental results are presented. Calligraphic poling will be used as a tool to create high efficiency nonlinear optical devices, as well as a tool to explore ferroelectric poling dynamics. Finally, in addition to LiNbO_3 , other z-cut ferroelectric materials, e.g. LiTaO_3 , can be domain engineered using calligraphic poling. x-Cut crystals can also be poled using a variation of calligraphic poling. Visualization of the domain growth could be useful for understanding of the internal processes in the ferroelectric materials.

Further experiments include generation of nonclassical states of light from periodically poled WGM resonators, and increasing efficiency of nonlinear optical processes in periodically poled WGM resonators. Outside of the context of nonlinear optics, domain engineering and visualization in ferroelectric materials could lead to new insights regarding the issue of domain wall propagation and charge fractionalization [16].

5. REFERENCES

1. G.A. Magel, M.M. Fejer, R.L. Byer "Quasi-phase-matched second-harmonic generation of blue light in periodically poled LiNbO_3 ", *Appl. Phys. Lett.* **56**, 108 — 110 (1990)
2. L.E. Myres, R.C. Eckardt, M.M. Fejer, R.L. Byer, W.R. Bosenberg, J.W. Pierce, "Quasi-phase matched optical parametric oscillators in bulk periodically poled LiNbO_3 ", *J. Opt. Soc. Am. JOSA B*, **12**, 2102 — 2116 (1995)
3. M. Houé, P.D. Townsend, "An introduction to methods of periodic poling for second harmonic generation", *J. of Phys. D: Appl. Phys.*, **28**, 1747 — 1763 (1995)
4. M. Yamada, "Electrically induced Bragg-diffraction grating composed of periodically inverted domains in lithium niobate crystals and its application devices", *Rev. of Sci. Instr.*, **71**, 4010 — 4016 (2000)

5. E.J. Lim, M.M. Fejer, F.L. Byer, W.J. Kozlovsky, "Blue light generation by frequency doubling in periodically poled lithium niobate channel waveguide", *Elec. Lett.*, **25**, Issue 11, 731 -- 732 (1989)
6. M.M. Fejer, G.A. Magel, D.H. Jundt, R.L. Byer, "Quasi-Phase-Matched Second Harmonic generation: Tuning and tolerances", *IEEE J. of Quan. Elec.*, **28**, No. 11, 2631 -- 2654 (1992)
7. N.G.R. Broderick, G.W. Ross, H.L. Offerhaus, D.J. Richardson, D.C. Hanna, "Hexagonally poled lithium niobate: A two dimensional nonlinear photonic crystal", *Phys. Rev. Lett.*, **84**, No. 19, 4345 -- 4384 (2000)
8. K.S. Zhang, T. Coudreau, M. Martinelli, A. Maitre, C. Fabre, "Generation of bright squeezed light at 10.6 μm using cascaded nonlinearities in a triply resonant cw periodically poled lithium niobate optical parametric oscillator", *Phys. Rev. A*, **64** (2001)
9. M. Yamada, N. Nada, M. Saitoh, K. Watanabe, "First order quasi-phase matched LiNbO₃ waveguide periodically poled by applying an external field for efficient blue second harmonic generation", *Appl. Phys. Lett.*, **62**, 435 -- 436 (1992)
10. R.G. Batchko, V.Y. Shur, M.M. Fejer, R.L. Byer, "Backswitch poling in lithium niobate for high-fidelity domain patterning and efficient blue light generation", *Appl. Phys. Lett.*, **75**, 1673 -- 1675 (1999)
11. V.Y. Shur, E.L. Romyantsev, E.V. Nikolaeva, E.I. Shishkin, E.V. Fursov, R.G. Batchko, L.A. Eyres, M.M. Fejer, R.L. Byer, "Nanoscale backswitched domain patterning in lithium niobate", *Appl. Phys. Lett.*, **76**, 143 -- 145 (2000)
12. H. Ishizuki, T. Taira, S. Kurimura, J.H. Ro, M. Cha, "Periodic poling in 3-mm-thick MgO:LiNbO₃ Crystals", *Japanese J. of Appl. Phys.*, **42**, 108 -- 110 (2003)
13. V.S. Ilchenko, A.A. Savchenkov, A.B. Matsko, L. Maleko, "Nonlinear Optics and Crystalline Whispering Gallery Mode Cavities", *Phys. Rev. Lett.*, **92**, No. 4043903 (2004)
14. M. Mohageg, D.V. Strekalov, A.A. Savchenkov, A.B. Matsko, V.S. Ilchenko, L. Maleki, "Calligraphic poling of lithium Niobate," *Opt. Express* **13**, No. 9 3408 (2005)
15. M. Mohageg, A.B. Matsko, A.A. Savchenkov, D. Strekalov, V.S. Ilchenko, L. Maleki, "Reconfigurable Optical Filter", *Elec. Lett.*, accepted for publication (2005)
16. R.E. Prange, "Conditions for charge fractionalization," *Phys. Rev. B* **26**, 991 (1982)
17. H.A. Eggert, B. Hecking, K. Buse, "Electrical fixing in near-stoichiometric lithium niobate crystals", *Opt. Lett.*, **29**, No. 21, 2476 -- 2478 (2004)
18. S. De Nicola, P. Ferraro, A. Finizo, S. Grilli, G. Coppola, M. Iodice, P. De Natale, M. Chiarini, "Surface topography of microstructures in lithium niobate by digital holographic microscopy", *Meas. Sci. and Tech.*, **15**, 961 -- 968 (2004)
19. V.S. Ilchenko, A.B. Matsko, A.A. Savchenkov, L. Maleki, "Low threshold parametric nonlinear optics with quasi-phase-matched whispering-gallery modes", *JOSA B*, **20**, No. 6, 1304 -- 1308 (2003)
20. M. Müller, E. Soergal, K. Buse, "Visualization of ferroelectric domains with coherent light", *Opt. Lett.* **28** 2515 -- 2517 (2003)
21. D.H. Jundt, "Temperature-dependant Sellmeier equation for the index of refraction, n_o , in congruent lithium niobate", *Opt. Lett.* **22**, 1553 -- 1555 (1997)